2007 IEEE International Conference on
Robotics and Automation
Roma, Italy, 10-14 April 2007

Integrated Estimation for Wheeled Mobile Robot posture, velocities, and wheel skidding perturbations

Chang Boon Low
Nanyang Technological University
School of Electrical and Electronics Engineering
Singapore 639798
cb@pmail.ntu.edu.sg

Danwei Wang*
Nanyang Technological University
School of Electrical and Electronics Engineering
Singapore 639798
edwwang@ntu.edu.sg

Abstract— **This paper presents a scheme for high-update rate Wheel Mobile Robot (WMR) posture, velocities, and perturbation estimation using Real-time Kinematic Global Positioning System (RTK-GPS) and inertial sensors for WMR control in the presence of wheel skidding and slipping. An outdoor estimation system based on Kalman Filtering combines the inertial measurements with centimeter accuracy RTK-GPS measurements to provide essential posture, velocities, and perturbation information. The particular contribution of this paper is in designing an estimation system to be able to deal with WMR control problems in the presence of wheel skidding and slipping. The experimental results suggest that with careful modelling of WMR, the estimation scheme is able to provide reliable and high update rate information for WMR control applications in the presence of wheel skidding and slipping.**

I. INTRODUCTION

Wheeled Mobile Robots control problems can be grouped into *path following*, *stabilization* and *trajectory tracking* [1], and many solutions to these problems have been proposed. However, most of these proposed control designs assume no wheel skidding and slipping.

In practice, wheel skidding and slipping effects are common since tire deformation is essential to provide longitudinal traction force for motion; hence, it is important to consider these factors in a WMR control design for safe and reliable maneuvers. Some works have been proposed to address the WMR control problems in the presence of wheel skidding and slipping [2], [3], [4]. However from the literature review, these control solutions impose restrictive assumptions either on the skidding perturbations or on the WMR's control inputs to achieve stability and performances. Recently, a control scheme has been proposed to address the issue [5], [6], [7], [8]. The control scheme exploits centimeter accuracy RTK-GPS measurements and inertial measurements to compute the skidding perturbations information which is utilized to achieve exponential converging solution based on the WMR kinematic model. However, the approach of perturbation computation only deploys observation equations which suffers from under utilization of these sensor data. Consequently, the low-update rate GPS measurements limits the control system's performance. Moreover, measurement noise has not been considered in these works.

To enhance information updating rate and reliability, the RTK-GPS measurements can be fused with other high-update rate navigation sensors to estimate the posture and perturbation information in a systematic way. These high-update rate navigation measurements must not be affected by the wheel skidding and slippage. This requirement suggests that Odometry methodology is unreliable to be used to estimate the vehicle posture. A review of navigation literature [9], [10] shows that GPS and inertial sensors have complementary properties, and they can be fused using Kalman Filter to provide high-update rate navigation information. Most importantly, these devices provide measurements that are not corrupted by wheel skidding and slipping effects. The combination of GPS and inertial sensors has also been utilized in automotive industry to estimate vehicle's sideslip angle for automobile stability control [11], [12], [13]. In these works, GPS doppler velocity measurements provided by a stand-alone GPS receiver is used to estimate the vehicle's sideslip and tire-slip angle. In WMR control problem in the presence of wheel skidding and slipping, the control system requires not only high-update rate perturbation information, but also high-update rate posture, e.g., the WMR's posture with respect to a global coordinate frame, which is not critical in automobile stability control applications. Other relevant work has also been found in [14] where a navigation system based on laser scanner and inertial navigation system was proposed for an autonomous underground load, haul, and dump truck. In the work, wheel skidding parameters of the vehicle are modelled as random white noise which may not be sufficiently accurate in representing the wheel skidding parameters.

RTK-GPS has also been used to compute the skidding parameters of a farm tractor for path-following problem [15], [16]. In these works, they utilized several versions of path following models for the estimation. However, these estimations suffer from several deficiencies. First, the estimators used a parameterized path following model for computing the perturbations. The computations utilize lateral deviation which requires accurate instantaneous curvilinear information to compute. A mild error in the position mea-

*Corresponding author: Prof Danwei Wang, School of EEE, Nanyang Technological University, Singapore 639798, Fax: (+65) 6793-3318, Email: edwwang@ntu.edu.sg

This work is partially supported by A*STAR SERC Grant No 0521160078, Singapore

surement could possibly lead to an erroneous and noisy estimates. Additionally, the update rates of these estimators are limited by the low-update rate GPS measurements. The perturbation estimator should be developed using a WMR's kinematic description rather than restrictive path-following models since the skidding parameters are properties of the WMR and should be problem independent.

In this paper, we proposed a kinematic estimator to provide reliable and high-update rate posture, velocities, and perturbations information for WMR control in the presence of wheel skidding effect. The WMR considered in this paper is a car-like WMR where control schemes have been proposed in [5], [6], [7], [8]. This article aims to demonstrate that the Kalman filters can be applied to estimate the WMR's posture, velocities, and kinematic perturbations for WMR control in the presence of wheel skidding and slipping. The remainder of this paper is organized as follows: Section II briefly describes the kinematic model of the robot. Section III presents the state-space modeling for the estimation. Section IV describes the estimation scheme, Section V presents the experimental results, and Section VI concludes the paper.

II. WMR Posture kinematic model

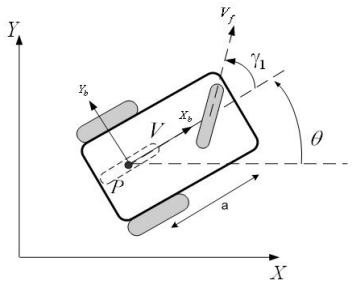

Fig. 1. Type (1,1) car-like WMR

In this paper, we consider a car-like WMR, as shown in Figure 1. This class of WMR is equipped with centered front steerable wheels and fixed parallel rear wheels. $\{X_b, Y_b\}$ denotes a body frame attached on the WMR reference point P and $\{X, Y\}$ represent the global coordinate frame. γ_1 denotes the WMR's front steering angle, a denotes the WMR's wheelbase, and θ represents the orientation of the WMR with respect to the $\{X\}$ axis. We define the vector $\xi = [x, y]^T$ as the coordinates of point P.

In the ideal case where no-skidding and no-slipping assumptions hold, a wheel's velocity is constrained along its wheel's plane axis. When these assumptions are not satisfied, the wheel's velocity deviates from its plane axis by a slip angle. To apply this characterization to the WMR, we let $\{\delta_1, \delta_2\}$ denote the front and rear wheels' slip angles as shown in Figure 2. V denotes the velocity of the reference point P, ψ denotes the orientation of the velocity with respect to the $\{X\}$ axis, V_l denotes the longitudinal velocity and V_y denotes the lateral velocity due to wheel skidding which is

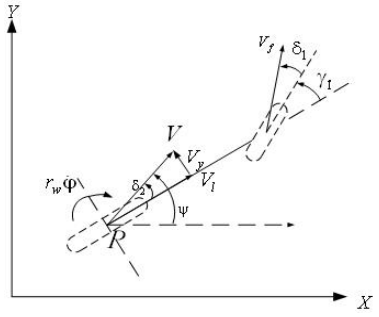

Fig. 2. Type (1,1) car-like WMR in the presence of skidding effects

related with the slip angle δ_2 by geometric relations

$$\sin\delta_2 = \frac{V_y}{V}, \quad \tan\delta_2 = \frac{V_y}{V_l}. \tag{1}$$

The posture kinematic model of the WMR in the presence of wheel skidding and slipping effects is

$$\dot{x} = V_l\cos(\theta) - V_y\sin(\theta) \tag{2}$$

$$\dot{y} = V_l\sin(\theta) + V_y\cos(\theta) \tag{3}$$

$$\dot{\theta} = \frac{V_l}{a}\tan(\gamma_1 + \delta_1) - \frac{V_y}{a}. \tag{4}$$

The WMR's longitudinal slippage d is related with the WMR's velocity control input $r_w\dot{\varphi}$ by $V_l = r_w\dot{\varphi} - d$. The control input of the WMR is $\mathbf{U}(t) = [r_w\dot{\varphi}\ \gamma_1]^T$ whereas the perturbations parameters due to wheel skidding and slipping are $\{V_y, d, \delta_1, \delta_2\}$. In brief, the estimation problem considered in this paper is to utilize the high-update rate inertial sensors measurements and the lower update rate RTK-GPS measurements to estimate the WMR's posture $\{x, y, \theta\}$, velocities $\{V_l, V_y\}$, and perturbation parameters $\{d, \delta_1, \delta_2\}$ at an update rate that the inertial sensors can provide.

III. Kinematic modeling for estimation

In this section, we derive a state-space model for Kalman filtering. The velocity of the WMR can be expressed as

$$\dot{\xi} = A(\theta)\eta \tag{5}$$

where

$$A(\theta) = \begin{bmatrix} \cos(\theta) & -\sin(\theta) \\ \sin(\theta) & \cos(\theta) \end{bmatrix}, \quad \eta = \begin{bmatrix} V_l \\ V_y \end{bmatrix}. \tag{6}$$

To relate $\dot{\xi}$ with acceleration, we differentiate equation (5). By some algebraic manipulations, we have

$$\dot{\eta} = \bar{P}\eta + u_a + w_a + \epsilon_a \tag{7}$$

where

$$\bar{P} = \begin{bmatrix} 0 & r \\ -r & 0 \end{bmatrix}, \quad u_a = \begin{bmatrix} a_x \\ a_y \end{bmatrix}, \quad \epsilon_a = \begin{bmatrix} \epsilon_{ax} \\ \epsilon_{ay} \end{bmatrix}. \tag{8}$$

u_a is the reference point acceleration measurements expressed in the WMR's body frame. w_a denotes the accelerometer measurement noise which is assumed to be

gaussian white with a sampled variance of $\{\sigma_{a,x}^2, \sigma_{a,y}^2\}$, ϵ_a is the accelerometer's bias, and r denotes the WMR's turning rate. Similarly, we can relate the gyroscope measurement with the WMR's orientation via

$$\dot{\theta} = r_m + w_r + \epsilon_r. \tag{9}$$

r_m represents the gyroscope measurement, ϵ_r is the gyroscope's bias, and w_r denotes gyroscope's measurement noise which is assumed to be zero mean gaussian white noise with sampled variance of σ_r^2. We consider the slow drifting biases $\{\epsilon_a, \epsilon_r\}$ are constant and known; hence, equations (5),(7),(9) can be written in the following state-space form.

$$\dot{\xi} = A(\theta)\eta \tag{10}$$
$$\dot{\eta} = \bar{P}\eta + u_a + w_a \tag{11}$$
$$\dot{\theta} = r_m + w_r \tag{12}$$

When GPS measurements (both position and velocities) are available, the observation equations that relate the measurements with the states (ξ, η) can be described by

$$z_x = x + v_x \tag{13}$$
$$z_y = y + v_y \tag{14}$$
$$z_{\dot{x}} = \cos\theta V_l - \sin\theta V_y + v_{\dot{x}} \tag{15}$$
$$z_{\dot{y}} = \sin\theta V_l + \cos\theta V_y + v_{\dot{y}} \tag{16}$$

where measurement noise $\{v_x, v_y, v_{\dot{x}}, v_{\dot{y}}\}$ are assumed to be zero mean and gaussian white with sampled variance $\{\sigma_x^2, \sigma_y^2, \sigma_{\dot{x}}^2, \sigma_{\dot{y}}^2\}$. Similarly, if an absolute orientation measurement is available, the observation equation of state θ is simply

$$z_\theta = \theta + v_\theta \tag{17}$$

where v_θ is also zero mean gaussian white noise with sampled variance σ_θ^2. Sensors that provide absolute orientation measurement are: magnetic compass, gyrocompass, and a two-antenna GPS system. Equations (10)-(12) and observation equations (13)-(17) lead to a continuous state-space model.

IV. WMR POSTURE, VELOCITIES, AND PERTURBATION ESTIMATION SYSTEM

A. Estimation system

Figure 3 shows the architecture of the estimation system based on Kalman filtering. At time k, the states $\{x, y, \theta, V_l, V_y\}$ are estimated by the Extended Kalman Filter (EKF). This is achieved by using the inertial, RTK-GPS, and absolute orientation measurements.

At any time instant where there is no absolute observation, the state prediction predicts the states by integrating the kinematic model (10)-(12) using the high bandwidth inertial measurements. In this manner, the prediction estimates has a maximum update rate that the inertial sensors can offer. However, integrating inertial measurements result the velocity and orientation estimate errors to grow linearly with time and the position error to grow quadratically with time

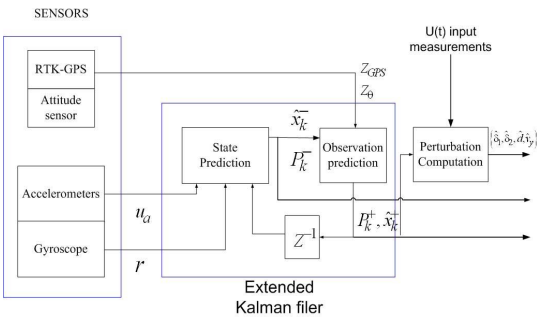

Fig. 3. Structure of the Estimation Scheme

[19]. The error growth rate depends on the quality of the inertial measurements. A high quality inertial sensors can provide estimates using integration without any online error calibration for a longer duration. At any time instant when the low-update rate absolute GPS and orientation measurements are available, the integration errors accumulated by the integration are reset by the observation prediction based on the respective absolute measurements and observation equations. Once the states $\{x, y, \theta, V_l, V_y\}$ are estimated, the scheme computes the skidding and slipping perturbations $\{\delta_1, \delta_2, d\}$ based on the states, control input $\mathbf{U}(t)$, and the WMR's kinematic model. The control inputs are usually known or measurable. For this configuration of WMR, the control inputs are the angular rotation rates of the rear wheels and the front steering angle. These inputs are measurable by high bandwidth sensors, e.g., incremental encoders and absolute encoder. In this way, the estimation system is able to provide posture, velocities, and perturbation estimates at an update rate that the inertial sensors can offer.

B. Discrete kinematic model

To implement the EKF, we discretize the continuous model (10)-(12), where the observation equations are sampled at a regular interval. The discrete state-space model of equations (10)-(12) can be established using first order *Euler* integration and is written in the form (18). A higher order integration may be used to enhance the accuracy of the discrete model. k denotes the discrete time index.

The discretized state transition vector equation is

$$\mathbf{x}_{k+1} = \mathbf{f}(\mathbf{x}_k, k) + \mathbf{w}_k \tag{18}$$

where

$$\mathbf{f}(\mathbf{x}_k, k) = \begin{bmatrix} x_k + \triangle t V_{l,k}\cos(\theta_k) - \triangle t V_{y,k}\sin(\theta_k) \\ y_k + \triangle t V_{l,k}\sin(\theta_k) + \triangle t V_{y,k}\cos(\theta_k) \\ V_{l,k} + \triangle t V_{y,k} r_k + \triangle t a_{x,k} \\ V_{y,k} - \triangle t V_{l,k} r_k + \triangle t a_{y,k} \\ \theta_k + \triangle t r_{m,k} \end{bmatrix}, \tag{19}$$

$\mathbf{x}_k = [x_k\ y_k\ V_{l,k}\ V_{y,k}\ \theta_k]^T$, and the process noise vector $\mathbf{w}_k = [0\ 0\ \triangle t w_{a,x}\ \triangle t w_{a,y}\ \triangle t w_r]^T$. The time-varying parameters $\{a_{x,k},\ a_{y,k},\ r_{m,k}\}$ at time k are provided by the

accelerometer and gyroscope. $\triangle t$ denotes the sample time of the discrete system. We assume the instantaneous yaw rate r_k is measurable by a low-noise gyroscope; hence, let $r_k = r_m$.

The observation vector $\mathbf{z}_k = [z_{x,k}\ z_{y,k}\ z_{\dot{x},k}\ z_{\dot{x},k}\ z_{\theta,k}]^T$ consists of absolute position, velocity and orientation readings. Vector $\mathbf{z}_k$ is related with the states $\mathbf{x}_k$ via the observation equations (13)-(17) sampled at time k which can be written as

$$\mathbf{z}_k = \mathbf{h}(\mathbf{x}_k) + \mathbf{v}_k, \tag{20}$$

where

$$\mathbf{h}(\mathbf{x}_k) = \begin{bmatrix} x_k \\ y_k \\ \cos\theta_k V_{l,k} - \sin\theta_k V_{y,k} \\ \sin\theta_k V_{l,k} + \cos\theta_k V_{y,k} \\ \theta_k \end{bmatrix}, \tag{21}$$

and observation noise $\mathbf{v}_k = [v_{x,k}\ v_{y,k}\ v_{\dot{x},k}\ v_{\dot{y},k}\ v_{\theta,k}]^T$.

C. State Prediction

The state prediction $\hat{\mathbf{x}}_{k+1}^-$ based on information up to time k is given by

$$\hat{\mathbf{x}}_{k+1}^- = \mathbf{f}(\hat{\mathbf{x}}_k, k). \tag{22}$$

The error covariance between the true state and the predicted state $\hat{\mathbf{x}}_{k+1}^-$ is given by

$$\mathbf{P}_{k+1}^- = \nabla\mathbf{f}(\hat{\mathbf{x}}_k)\mathbf{P}_k\nabla\mathbf{f}^T(\hat{\mathbf{x}}_k) + \mathbf{Q}_k. \tag{23}$$

$\nabla\mathbf{f}(.)$ denotes the Jacobian of $\mathbf{f}(.)$ at time k, and $\mathbf{Q}_k$ is the covariance matrix of the discretized noise vector $\mathbf{w}_k$. Note that $\hat{\mathbf{x}}_k$ and $\mathbf{P}_k$ are chosen as $\hat{\mathbf{x}}_k^+$ and $\mathbf{P}_k^+$ if there are measurements available at time k; and $\hat{\mathbf{x}}_k$ and $\mathbf{P}_k$ are chosen as $\hat{\mathbf{x}}_k^-$ and $\mathbf{P}_k^-$ if there is no measurement $\mathbf{z}_k$ available at time k;

D. Observation Prediction

Assuming that there is a predicted state $\hat{\mathbf{x}}_k^-$, we have the predicted observation

$$\hat{\mathbf{z}}_k = \mathbf{h}(\hat{\mathbf{x}}_k^-). \tag{24}$$

Suppose the measurements $\mathbf{z}_k$ at time k are available, the prediction observation error which is also known as residual is defined as $\boldsymbol{\alpha}_k = \mathbf{z}_k - \hat{\mathbf{z}}_k$ with the covariance

$$\mathbf{S}_k = \nabla\mathbf{h}(\hat{\mathbf{x}}_k^-)\mathbf{P}_k^-\nabla\mathbf{h}^T(\hat{\mathbf{x}}_k^-) + \mathbf{R}_k. \tag{25}$$

$\nabla\mathbf{h}(.)$ denotes the Jacobian of $\mathbf{h}(.)$ where $\mathbf{R}_k$ is the covariance matrix of the measurements noise. The state estimate and covariance update equations of a EKF is as follows:

$$\hat{\mathbf{x}}_k^+ = \hat{\mathbf{x}}_k^- + \mathbf{K}_k(\boldsymbol{\alpha}_k) \tag{26}$$

where $\mathbf{K}_k$ is the Kalman gain given by

$$\mathbf{K}_k = \mathbf{P}_k^-\nabla\mathbf{h}^T(\hat{\mathbf{x}}_k^-)\mathbf{S}_k^{-1} \tag{27}$$

and the state estimate covariance matrix is

$$\mathbf{P}_k^+ = (\mathbf{I} - \mathbf{K}_k\nabla\mathbf{h}(\hat{\mathbf{x}}_k^-))\mathbf{P}_k^-. \tag{28}$$

To improve the reliability of the estimation scheme, a validation mechanism under the framework of Kalman filter can be applied to inspect the measurements so that occasional bad measurements will not affect the estimates [18]. This approach has been implemented to improve the reliability of the estimation system [19]. Here, we may also implement this validation mechanism to increase the integrity of the estimator. To implement the validation gate, a threshold λ_i which to be selected by the designer such that

$$\text{Prob}\{\alpha_i^2 > \lambda_i(S_i)\} = \mu_i \tag{29}$$

where α_i is the ith element of $\boldsymbol{\alpha}_k$, S_i is the ith diagonal term of matrix $\mathbf{S}$, and a constant $\mu_i \in (0,1)$ is usually quite small. Then if condition

$$\alpha_i^2 > \lambda_i(S_i) \tag{30}$$

is satisfied, the corresponding measurement will be declared as faulty measurement. Note that the parameter λ_i should be tuned by experimental trials. In the case where the measurements $\mathbf{z}_k$ are not available or faulty, the estimator simply applies state prediction to estimate using inertial measurements until the next absolute measurements $\mathbf{z}_k$ arrive.

E. Perturbation computation

With the knowledge of $\hat{\mathbf{x}}_k$, whether is by state prediction or by observation prediction, we can make use of the estimate to compute the kinematic perturbations $\{d, \delta_1, \delta_2\}$ at time k using the following equations.

$$\hat{d} = r_w\dot{\varphi} - \hat{V}_l \tag{31}$$

$$\hat{\delta}_1 = \tan^{-1}\left(\frac{r_m a + \hat{V}_y}{\hat{V}_l}\right) - \gamma_1 \tag{32}$$

$$\hat{\delta}_2 = \tan^{-1}\frac{\hat{V}_y}{\hat{V}_l} \tag{33}$$

Since control input $\mathbf{U}(t)$ of the WMR is assumed to be known or measurable, and the the slip angles satisfy $|\delta_i| < \frac{\pi}{2}$ for $i = 1, 2$, the perturbations can be uniquely computed using equations (32) and (33).

V. Experiments

A. Experimental setup

Experiment was conducted in an open and flat area at our school. The open area was selected so that the effects of inertial sensor bias due to gravitational effect was minimized, and the consistency of the line of sights between the receiver and the GPS satellites was maintained during the trial. The proposed algorithm was tested on a car-like mobile robot platform named *Cycab* (see Fig. 4). The mobile robot has four wheels which are driven by four independent DC motors. Two incremental encoders are fitted on the rear DC motors to measure the WMR velocity input $r_w\dot{\varphi}$. An absolute encoder is installed on the WMR's steering system to measure the steering angle γ_1. The WMR is equipped with a MS-750 RTK-GPS receiver which is able to provide both position and velocities measurements simultaneously. The accuracies of the position and velocity measurements

Fig. 4. A Type (1,1) car-like WMR

are $1\sigma = 0.02m$ and $1\sigma = 0.03\text{ms}^{-1}$ respectively. We let the $\{X, Y\}$ axes of the global coordinate system be the East and North axes. Additionally, a KVH RA1100 Fibre Optic gyroscope and a CXL01LF3 tri-axial accelerometer are attached on the WMR's reference point P to provide high-update rate inertial information. The low-noise gyroscope has a low measurement error of $1\sigma = 0.1$deg/sec and the accelerometer's measurement error is $1\sigma = 0.01\text{ms}^{-2}$. A Pentium PC with Window operating system hosts the vehicle control software. The software is written using Visual C++ to communicate with the Cycab's onboard for steering and driving actions. The software is interfaced with a 12-bits DAQ card to acquire the signals from the inertial sensors and the absolute encoder. The GPS receiver is programmed to provide measurements at an update rate of 10Hz where the higher update rate sensors were sampled at 20Hz. The WMR is not equipped with an absolute orientation sensor that measures the WMR's orientation θ. Since, the WMR is to maneuver at a low speed about $V_l = 1.0$ ms^{-1}, the rear slip angle δ_2 of the WMR is negligent; hence, we let the velocity orientation ψ measurement provided by the GPS receiver be the absolute WMR orientation measurement z_θ for the estimation scheme. Note that the ψ measurement error is inversely proportional to the receiver's velocity [11].

B. Experimental results

During the trial run, the WMR maneuvered in a circular path while the sensors data was collected for the fusion. Both velocity and position measurements are provided by the RTK receiver and are used in this fusion. Figure 5 shows the position and velocity estimates. Figure 6 depicts the kinematic perturbations estimates computed by equations (31) and (32). These estimates have an update rate of 20Hz. The spikes occurred in $\hat{\delta}_1$ estimate during $0 < t < 3$ sec were due to the zero velocity when the WMR was stationary. We can simply let $\hat{\delta}_1 = 0$ when the robot is stationary since there should have no wheel skidding when the WMR is motionless. The sharp spikes of the $\hat{d}$ estimates were due to the high frequency incremental encoder measurement noise which can be eliminated by implementing a low-pass

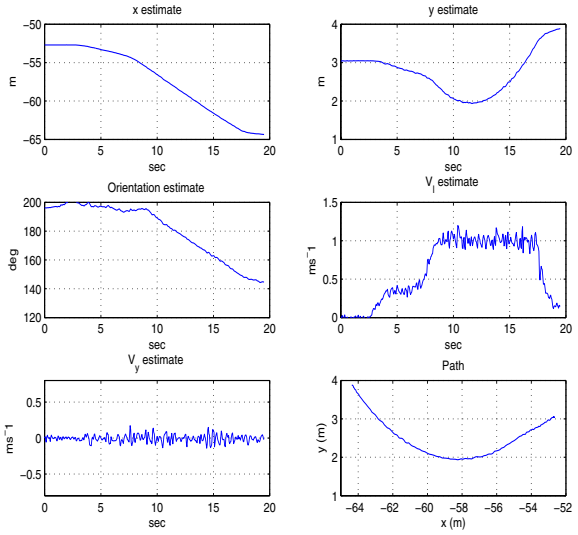

Fig. 5. Posture, velocities, and Perturbation estimates

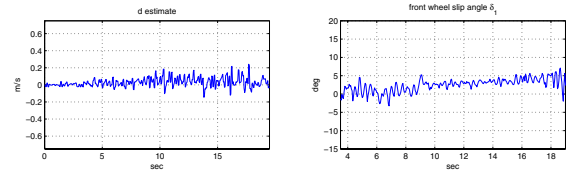

Fig. 6. Posture, velocities, and Perturbation estimates

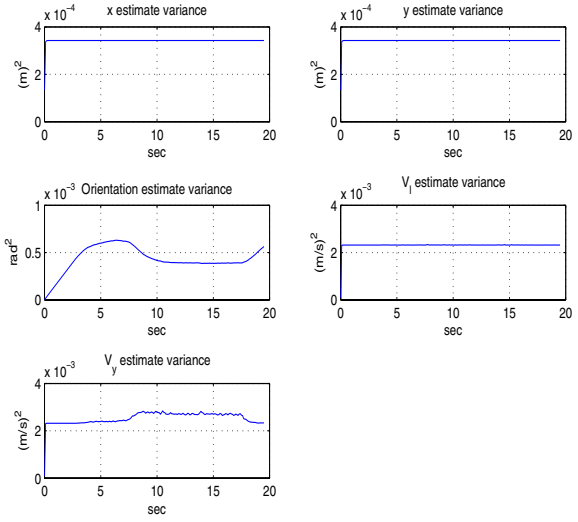

Fig. 7. Variances of the estimates

filter. Figure 7 depicts the approximated variances of the estimates computed by the filter. The bounds of these error variances indicate that the EKF is well-behaved and stable. Finally, Figure 8 presents the measurement residuals of the estimator with 2σ plot. The whiteness and zero bias of these

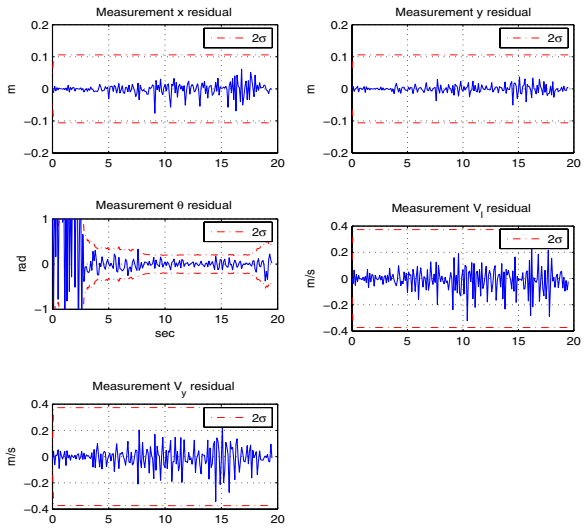

Fig. 8. Measurement residuals

residual indicates the consistency of the filter. The large spikes occasionally occurred in the orientation measurement residual is mainly due to the initial noisy measurement z_θ when the WMR is stationary. The sudden increments of the position and velocity residuals during the run were caused by the GPS multipath error when the WMR crossed some of the palm trees along the path. Due to the space limitation, the measurement rejection mechanism is not implemented to rejected the occasional faulty measurements. Nevertheless, a threshold level λ of condition (30) may be defined for the measurement validation condition to reject these faulty GPS measurements whenever the residuals exceeds the predefined threshold level. The validation implementation will enhance the reliability of the estimation system, especially in areas where multipath error is dominant. These results show the effectiveness of the estimator.

VI. Conclusions

This paper has developed a reliable and high-update rate estimation system to provide critical posture, velocities, and kinematic perturbation estimates in the presence of wheel skidding and slipping for a car-like WMR. A kinematic estimator is proposed to combine the low-update rate RTK-GPS measurements with high-update rate inertial measurements based on Kalman Filter. In this way, the update rate of the estimates is now limited by the inertial sensor's bandwidth instead of the low-update rate GPS measurements. One advantage of this kinematic estimator is that the inertial parameters of the robot, which are usually unknown, are not required to estimate the kinematic perturbations. Another advantage is that the system can continue to provide estimates using inertial sensors for short durations where the GPS signals are unavailable or corrupted by high frequency multipath error. With these high-update rate estimates, WMR control laws that are designed to compensate the kinematic perturbations due to wheel skidding and slipping can be applied more effectively for precise automatic maneuvers.

References

[1] A. De Luca and G. Oriolo, "Modeling and control of nonholonomic mechanical system," *Kinematics and dynamics of multi-body system*, Springer-Verlag, pp: 278-342, 1995.

[2] B. d'Andréa-Novel and G. Campion and G. Bastin, "Control of Wheeled Mobile Robots Not Satisfying ideal velocity constraints: A Singular Perturbation Approach," *The International Journal of Robust and Nonlinear control*, vol. 5, pp. 243-267, 1995.

[3] C. Canudas de Wit and H. Khennouf, "Quasi-Conjtinuous stabilizing controllers for nonholonomic systems: design and robustness considerations," *Proceedings of the 3rd European Control Conference*, pp. 2630-2635, 1995.

[4] W. E. Dixon and D. M. Dawson and E. Zergeroglu, "Robust Control of a mobile robot system with kinematic disturbances," *Proceedings of the 2000 IEEE International Conference on Control Applications*, pp. 437-442, 2000.

[5] C. B. Low and D, Wang, "Robust Path following control of a car-like Wheeled Mobile Robot in the presence of skidding," *Proceedings of IEEE/ICM International Conference of Mechatronics*, July, Taipei, 2005.

[6] C. B. Low and D, Wang, "GPS-based Path following Control for a car-like Wheeled Mobile Robot with skidding and slipping," *IEEE Transaction on Control Systems Technology*, Submitted for review, 2006.

[7] D. Wang and C. B. Low, "Tracking Control of a car-like Wheeled Mobile Robot in the presence of skidding effects," *Proceedings of 2005 IEEE/CIRAS Computational Intelligence, Robotics and Autonomous Systems*, Dec, Singapore, 2006.

[8] C. B. Low and D, Wang, "GPS-based Tracking Control for a car-like Wheeled Mobile Robot with skidding and slipping," *IEEE/ASME Transaction on Mechantronics*, Submitted for review, 2006.

[9] E. Abbott and D. Powell, "Land-vehicle Navigation Using GPS," *Proceedings of IEEE*, vol. 87, No. 1, pp: 145-162, Jan, 1999.

[10] B. Barshan and H. F. Durrant-Whyte, "Inertial Navigation Systems for Mobile Robots," *IEEE Transactions on Robotics and Automation*, vol. 11, No. 3, pp: 328-342, 1995.

[11] D. M. Bevly, "Global positioning system (GPS) a low-cost velocity sensor for correcting inertial sensor error on ground vehicles," *Journal of Dynamic Systems, Measurement, and Control*, vol. 126, pp: 255-265, 2004.

[12] D. M. Bevly and J. C. Gerdes and C. Wilson and G. Zhang, "The use of GPS based velocity measurement for improved vehicle state estimation," *in IEEE Proceeding of the American Control Conference*, vol. 4, pp: 2538-2542, June, 2000.

[13] D. M. Bevly and R. Sheridan and J. C. Gerdes, "Integrating INS sensors with GPS velocity measurements for continuous estimation of vehicle sideslip and tire cornering stiffness," *in IEEE Proceeding of the American Control Conference*, vol. 4, pp: 25-30, June, 2000.

[14] S. Scheding and G. Dissanayake and E. Nebot and H Durrant-Whyte, "Slip Modeling and Aided Inertial Navigation of an LHD," *Proceeding of 1997 International Conference of Robotics and Automation*, pp: 1904-1909, New Mexico, 1997.

[15] R. Lenain and B. Thuilot and C. Cariou and P. Martinet, "Adaptive Control for car like vehicles guidance relying on RTK GPS: rejection of sliding effects in agricultural applications," *Proceeding of 2003 IEEE International Conference on Robotics and Automation*, pp: 115-120, Taipei, 2003.

[16] R. Lenain and B. Thuilot and C. Cariou and P. Martinet, "A new nonlinear control for vehicle in sliding conditions: Application to automatic guidance of farm vehicles using RTK GPS," *Proceeding of 2004 IEEE International Conference on Robotics and Automation*, pp: 4381-4386, 2004.

[17] B. d'Andréa-Novel and G. Campion and G. Bastin, "Control of nonholonomic wheeled mobile robots by state feedback linearization," *The International Journal of Robotics Research*, vol. 14, pp. 543-559, Dec. 1995.

[18] J. Farrel, The Global Positioning System and Inertial Navigation System, *McGraw-Hill*, 1999.

[19] S. Sukkarieh and E. M. Nebot and H. F. Durrant Whyte, "A Hight Integrity IMU/GPS Navigation Loop for autonomous Land vehicle Application," *IEEE Transactions on Robotics and Automation*, vol. 15, no. 3, pp. 572-578, June, 1999.